Skin Optics

M. J. C. VAN GEMERT, STEVEN L. JACQUES, H. J. C. M. STERENBORG, AND W. M. STAR

(Invited Paper)

***Abstract*—Quantitative dosimetry in the treatment of skin disorders with (laser) light requires information on propagation of light in the skin related to the optical properties of the individual skin layers. This involves the solution of the integro-differential equation of radiative transfer in a model representing skin geometry, as well as experimental methods to determine the optical properties of each skin layer. These activities are unified under the name skin optics. This paper first reviews the current status of tissue optics, distinguishing between the cases of: dominant absorption, dominant scattering, and scattering about equal to absorption. Then, previously published data as well as some current unpublished data on (human) stratum corneum, epidermis and dermis, have been collected and/or (re)analyzed in terms of absorption coefficient, scattering coefficient, and anisotropy factor of scattering. The results are that the individual skin layers show strongly forward scattering (anisotropy factors between 0.7 and 0.9). The absorption and scattering data show that for all wavelengths considered scattering is much more important than absorption. Under such circumstances, solutions to the transport equation for a multilayer skin model and finite beam laser irradiation are currently not yet available. Hence, any quantitative dosimetry for skin treated with (laser) light is currently lacking.**

INTRODUCTION

TREATMENT of skin disorders with light makes use of absorption of photons by chromophores present in viable cells of either the epidermis or the dermis. Optimizing such treatments requires quantitative knowledge of the fraction of incident light that reaches the target chromophore, its ability to absorb that light, and the short and long term biological response of the (host) tissue.

The present analysis of skin optics will concentrate upon relations for the fluence rate distribution of light within the skin, related to the absorbing and scattering properties of the various skin components, in response to incident irradiance. If successful, quantitative light dosimetry can be introduced in, e.g., PUVA for psoriasis, photodynamic therapy of cancer, portwine stain coagulation, and photodynamic therapy for jaundice in newborns.

At present, a rigorous theory is far from being available, partly because skin is irregularly shaped, has hair follicles and glands, is inhomogeneous, multilayered, and has anisotropic physical properties. So any fruitful attempt to understand skin optics requires a considerably simplified model for the skin. A diagram of the skin and a simplified model consisting of epidermis and dermis as two plane parallel layers with isotropic physical properties is shown in Fig. 1. The layers are assumed to have the same refractive index ($n \sim 1.37$–1.5 [1]) but a different number density of absorbers and scatterers that are randomly distributed over the volume. As a consequence, wavelength dependent absorption and scattering coefficients (mm^{-1}) can be assigned to both the epidermis and dermis. Blood may either be explicitly taken into account (see Fig. 4 below) or it may be assumed to be homogeneously distributed in the dermis (Fig. 1); this latter assumption will influence the dermal absorption coefficient at certain wavelengths but (presumably) hardly the scattering coefficient. An additional optical parameter is the scattering phase function, expressing the probability density function that a photon moving in direction s is scattered into another direction s'. Within the concepts of such a model, propagation of light can be described by radiative transfer theory which originates from astrophysics [2]. This theory requires that the scatterers are far enough apart to scatter independently from each other. An additional simplification used here is that polarization effects are neglected. Despite the simple model described in Fig. 1, two complicating factors remain. First, a general (analytical) solution of the integro-differential equation of radiative transfer is not available under all conditions relevant for skin treatments. Solutions are available under restricted conditions only such as, e.g., uniform irradiation or when either absorption or scattering strongly dominates. Second, determination of the optical parameters

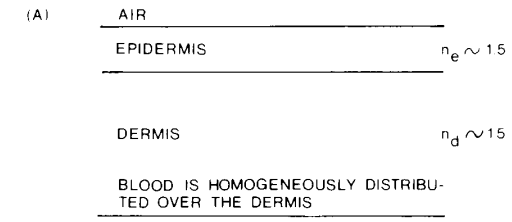

Fig. 1. Schematic model of skin with plane parallel epidermal and dermal layers. Each layer is homogeneous and has isotropic physical properties. Absorption and scattering are introduced by assuming a random but homogeneous distribution of absorbers and scatterers over the volume. Local scattering can be anisotropic. For convenience, blood is assumed here to be homogeneously distributed over the dermal volume. The refractive indexes of epidermis and dermis are considered identical. A number of 1.5 is mentioned for convenience.

Manuscript received December 5, 1988; revised May 1, 1989.

M. J. C. van Gemert and H. J. C. M. Sterenborg are with the Laser Centre, Academic Medical Centre, Amsterdam, The Netherlands.

S. L. Jacques is with Laser Biology Research Laboratory, The University of Texas/M. D. Anderson Cancer Center, Houston, TX 77030.

W. M. Star is with the Department of Clinical Physics, Dr. Daniel den Hoed Cancer Center, Rotterdam, The Netherlands.

IEEE Log Number 8931098.

(absorption, scattering, and phase function) requires not only the solution to the transport equation (or a suitable approximation) for an experimental geometry (e.g., a thin slab of tissue) but also an inverse solution that relates measurements such as reflection and transmission to the optical properties. Such methods have only been developed recently, usually under conditions that scattering dominates over absorption (so-called diffusion approximation).

The purpose of this paper is to review the status of tissue optics (solutions to the transport equation as well as experimental methods to measure the optical properties involved), and collect previously published as well as currently unpublished information on skin optical parameters, rearranged if necessary according to present day knowledge.

General Aspects of Transport of Light in Tissue

Assume collimated light normally incident upon a slab of turbid material with refractive index $n > 1$. Due to the mismatch in refractive index a small portion of the incident beam is specularly reflected, also called Fresnel reflection (4 percent for $n = 1.5$). The remaining 96 percent enters the tissue where it is attenuated due to absorption and scattering. Photons scattered out of the collimated beam initially propagate in (random) directions described by the phase function. These scattered photons contribute to a diffuse distribution of light in the tissue that extends beyond the boundaries of the collimated incident beam. A back scattered photon from the diffuse part of the light distribution that reaches the tissue–air boundary at an angle with the inward normal larger than the so-called critical angle for total reflection, is reflected back into the tissue. The critical angle is defined as the arcsine of $1/n$, so arcsin $(1/1.5) = 41.8°$ for $n = 1.5$. This process of total internal back-reflection against the tissue–air boundary for perfectly diffuse light leads to a 55 percent theoretical diffuse back-reflectance for $n = 1.5$ [1]. However, a much smaller diffuse back-reflectance coefficient may be more appropriate for laser irradiated skin because light close to boundaries may not be perfectly diffuse, but more forward directed.

The phase function for scattering $p(s, s')$ representing the albedo times the probability density function that a photon is scattered from direction s into direction s' depends only on the angle θ between s and s' due to the assumption that the scatterers are randomly distributed over the tissue volume, expressing that the tissue lacks spatially correlated structures. Thus,

$$p(s, s') = p(\theta). \tag{1}$$

Various theoretical phase functions considered for tissue are illustrated in Fig. 2. Isotropic scattering shown in Fig. 2(a) is represented as a constant

$$p(s, s') = \text{constant}. \tag{2a}$$

Slightly forward scattering can be represented by the first two moments of the phase function (see, e.g., Ishimaru [3], p. 177).

$$p(\theta) = \text{constant}\,[1 + 3g \cos\theta] \tag{2b}$$

where g is the mean cosine of the scattering angle (called anisotropy factor), arbitrarily chosen as $g = 1/6$ for depiction in Fig. 2(b). Isotropic scattering has $g = 0$; purely forward scattering $g = 1$, and purely backward scattering $g = -1$. Forward scattering according to the so-called Henyey–Greenstein phase function [4], [5, p. 307] is presented in Fig. 2(c)

$$p(\theta) = \left(\frac{\sigma_s}{\sigma_s + \sigma_a}\right) \frac{(1 - g^2)}{(1 + g^2 - 2g \cos\theta)^{3/2}} \tag{2c}$$

where σ_a, σ_s are the absorption and scattering coefficients (mm^{-1}). An approximation to (2c) shown in Fig. 2(d) is

$$p(\theta) = \left(\frac{\sigma_s}{\sigma_s + \sigma_a}\right) [2g\delta(1 - \cos\theta) + (1 - g)]. \tag{2d}$$

The first term indicates strongly forward peaked scattering and the second term isotropic scattering. Equations (2c) and (2d) are identical in their first two moments, that is

$$\frac{1}{2}\int_{-1}^{1} p(\cos\theta)\, d(\cos\theta) = \frac{\sigma_s}{\sigma_s + \sigma_a} \tag{3a}$$

$$\frac{1}{2}\int_{-1}^{1} \cos\theta\, p(\cos\theta)\, d(\cos\theta) = g\left(\frac{\sigma_s}{\sigma_s + \sigma_a}\right). \tag{3b}$$

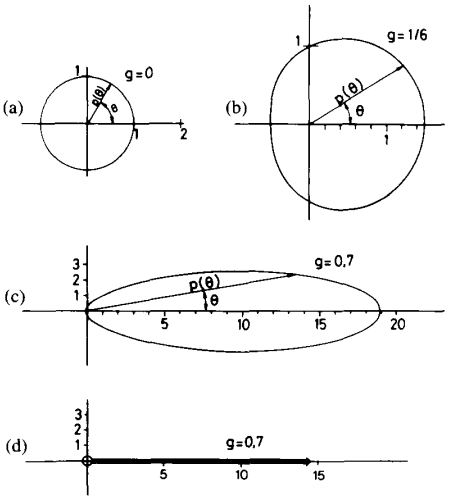

Fig. 2. Examples of phase functions $p(\theta)$. (a) Isotropic scattering, equation (2a). (b) Forward scattering, equation (2b) using an example of the first two moments of the phase function expansion in Legendre polynomials with $g = 1/6$. (c) The Henyey–Greenstein phase function, equation (2c), for $g = 0.7$. (d) An approximation to the Henyey–Greenstein phase function, identical in the first two moments, equations (2d) and (3).

Equation (3a) is the normalization condition imposed on the phase function. Both phase functions (2c) and (2d) have been used to characterize scattering of tissue (see below). The ratio $[\sigma_s/(\sigma_s + \sigma_a)]$ is called the albedo for single particle scattering.

Strong Absorption

For some (laser) wavelengths in the UV (e.g., at the ArF excimer laser wavelength at 193 nm) and the IR (Er-YAG laser at 2.94 μm; the CO_2 laser at 10.6 μm) tissue absorption may be substantially larger than scattering. Transport theory is then simple. The fluence rate in the tissue decreases exponentially with increasing depth according to

$$I_c(z, r) = I_L(r)\,(1 - r_{sp})\,e^{-\sigma_a z} \tag{4}$$

where $I_L(r)$ (watt m^{-2}) is the radial profile of the incident laser beam, $I_c(z, r)$ (watt m^{-2}) is the fluence rate in the tissue at coordinates z, r, and r_{sp} is the specular reflection coefficient (Fresnel reflection). Equation (4) is called Beer's law.

Experimentally, σ_a can be determined by measuring the transmittance (T) through a slab of material, with thickness t. From (4) this yields

$$\sigma_a = \frac{1}{t} \ln\left(\frac{1}{T}\right) \tag{5}$$

and T defined as

$$T = \frac{I_c(t)}{I_L(1 - r_{sp})}. \tag{6}$$

An experimental problem can be that thickness t should be extremely small when σ_a is large. For example, soft tissue has at the 10.6 μm wavelength of a CO_2 laser an absorption coefficient of approximately 60 mm^{-1}. In this case a thickness of $t = 38$ μm yields a 10 percent transmittance.

Strong Scattering

Between about 300 and 1000 nm nonpigmented tissues have scattering dominating over absorption. Under these circumstances the transport equation can be approximated by a diffusion equation in the diffuse light fluence rate $\phi_d(z, r)$ (watt m^{-2}), defined as the total amount of diffuse light power that passes through a small sphere located at (z, r) divided by the cross sectional area of that sphere. Under conditions of cylindrical symmetry the diffusion equation reads

$$\left[\frac{d^2\phi_d(z, r)}{dz^2} + \frac{d^2\phi_d(z, r)}{dr^2} + \frac{1}{r}\frac{d\phi_d(z, r)}{dr}\right] - 3\sigma_a[\sigma_a + \sigma_s(1 - g)]\,\phi_d(z, r) = -3\sigma_s[\sigma_s + (1 + g)\,\sigma_a]\,I_c(z, r) \tag{7}$$

where the first term on the left-hand side represents diffusion losses in the z and r directions (for cylindrical symmetry) which gives the name: diffusion equation. The right-hand side term involves the collimated laser beam attenuated by absorption and scattering $I_c(z, r)$ which is the source for the diffuse light distribution. Note that the phase function for scattering is here represented by the anisotropy factor g, the first moment of the phase function, (3b). Equation (7) can be solved analytically or numerically with appropriate boundary value conditions such as the specular reflectance of the collimated source and internal reflection of diffuse light at tissue–air interfaces; see, e.g., Groenhuis *et al.* [6] and Keijzer *et al.* [7]. The total fluence rate, $\phi(z, r)$, is the sum of the collimated and the diffuse components

$$\phi(z, r) = \phi_c(z, r) + \phi_d(z, r) \tag{8}$$

where $\phi_c(z, r) = I_c(z, r)$. Details of the derivation can be found in Ishimaru [3] and Groenhuis *et al.* [6]. For an infinite laser beam diameter (uniform irradiation of a semi-infinite slab), (7) can be rewritten as a set of first order differential equations in the diffuse forward and backward fluxes. This set can be solved analytically [8]–[10].

Solutions of (7) and (8) for $\sigma_a = 0.2$ mm^{-1}, $\sigma_s = 18.8$ mm^{-1}, and $g = 0.8$, which is a set of values that approximates *in vitro* dermal tissue at 633 nm wavelength [11] are shown in Fig. 3. A radially uniform intensity beam, radius w_L, was used. These results show that if w_L is large, $\phi(z = 0, r = 0)$ can be 3.3 times larger than the incident irradiance due to back scattering. This factor of 3.3 drops to 1 when w_L tends to zero. In other words, the viable light intensity distribution *inside* the tissue that is available for therapeutic benefits is a complicated function of σ_a, σ_s, g, *and* w_L. This makes any quantitative dosimetry extremely hard, especially because the relationships are not obvious.

In addition, for a multilayer (skin) model (7) has only been solved for uniform irradiation of a semi-infinite slab [3, pp. 216–219], [12]. A result of a four-layer skin model (from [12]) is shown in Fig. 4. The optical data used are from the present paper (Fig. 8 below). This four-layer skin model has been used to analyze portwine stain laser treatment [13], explicitly requiring a blood layer plexus. It therefore differs from the more general skin model of Fig. 1. For a finite laser beam a multilayer solution has not been published, but progress is being made with finite element and Monte Carlo models. The problem is that the second layer not only has an incident attenuated collimated beam, but also an incident diffuse beam from the first layer. In turn, the first layer, at the interface with the second, now has the back-reflected diffuse beam incident as well. As curves similar to Fig. 3 are not yet available for the skin model of Fig. 1 irradiated with a finite laser beam, any quantitative multiple layer dosimetry for skin treated with laser light is only possible when the laser spot is much larger than the penetration depth. In this case, the one-dimensional optical analysis provides an accurate estimate of fluence rate as a function of depth at the center of the beam. Fluence rate can be used to calculate the rate of heat generation in the tissue and then temperature can be calculated using the heat conduction equation.

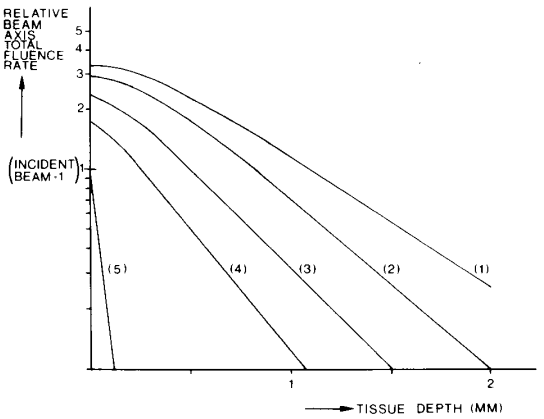

Fig. 3. Total fluence rate as a function of tissue depth z at $r = 0$ according to the diffusion model, equations (7) and (8), and optical parameters $\sigma_a = 0.2\ \text{mm}^{-1}$, $\sigma_s = 18.8\ \text{mm}^{-1}$, and $g = 0.8$ representing dermal tissue at 633 nm [11]. Beam diameters ($2w_L$) are: 1) infinite, 2) 2 mm, 3) 1 mm, and 4) 0.5 mm: curve 5) represents the collimated beam, attenuated according to $\exp[-(\sigma_a + \sigma_s)z]$. The laser beam has uniform irradiance: $I_c(z = 0, r) = 1$ for $r \leq w_L$ and $I_c(z = 0, r) = 0$ for $r > w_L$. Index mismatching has been used.

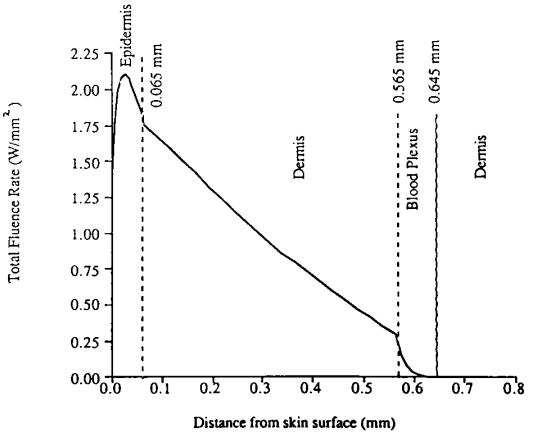

Fig. 4. Total fluence rate (watt/cm^2) versus depth from skin surface (mm) for a four-layer skin model. Refractive index matching with $n = 1.33$ is assumed for all layers. A collimated beam, of infinite dimension is assumed with 1 watt/mm^2 irradiance at 577 nm wavelength. Input data were as follows (Fig. 8). Epidermis: thickness 0.065 mm, $\sigma_{ae} = 3.8\ \text{mm}^{-1}$, $\sigma_{se} = 50\ \text{mm}^{-1}$, $g_e = 0.786$. Dermis: thickness 0.5 mm (upper dermis) and 0.3 mm (lower dermis), $\sigma_{ad} = 0.3\ \text{mm}^{-1}$, $\sigma_{sd} = 21.7\ \text{mm}^{-1}$ (Jacques' value, Fig. 8), $g_d = 0.81$. Blood: thickness 0.08 mm, $\sigma_{ab} = 37.6\ \text{mm}^{-1}$, $\sigma_{sb} = 0.96\ \text{mm}^{-1}$, $g_b = 0$.

In calculating the curves of Figs. 3 and 4, we have assumed numbers for σ_a, σ_s, and g are available. Actually, reliable methods to measure these parameters for strongly scattering materials are only currently being developed. Determination of the three independent parameters σ_a, σ_s, and g requires three independent measurements. Usually, one measurement is σ_t, the collimated attenuation coefficient for a thin slab of tissue [14]. The other two measurements refer to properties measured with the diffuse part of the light. One possibility is to measure the diffuse reflectance (R_d) and transmittance (T_d) of a slab of tissue with thickness t (e.g., in an integrating sphere geometry). First, these measurement yields parameters K, S via

$$S = \frac{1}{bt}\ln\left[\frac{1 - R_d(a - b)}{T_d}\right] \qquad K = S(a - 1) \tag{9a}$$

$$a = \frac{1 - T_d^2 + R_d^2}{2R_d} \qquad b = \sqrt{a^2 - 1} \tag{9b}$$

where K, S are absorption and scattering parameters of the Kubelka–Munk formalism [10]. Second, S and K have been related to the optical parameters by [15]

$$S = \tfrac{3}{4}\sigma_s(1 - g) - \tfrac{1}{4}\sigma_a \tag{10a}$$

$$K = 2\sigma_a. \tag{10b}$$

Adding the measured collimated attenuation coefficient σ_t

$$\sigma_t = \sigma_a + \sigma_s \tag{10c}$$

yields in a straightforward way to values of σ_a, σ_s, and g. Similar methods have been worked out by Marijnissen *et al.* [8], [9] and by Jacques and Prahl [16]. We recall, however, that scattering has to dominate over absorption [$\sigma_s(1 - g) >> \sigma_a$]. Below, [see (12)] relations between S, K and σ_a, σ_s, and g are presented that are more accurate than those of (10). In fact, (10) represent (12) in the limit that $\sigma_a/[\sigma_s(1 - g)]$ tends to zero.

Scattering About Equal to Absorption

In this situation no simplified solution to the transport equation [(11) below] is currently available and in order to find fluence rate distributions in tissue this equation needs to be completely solved. The transport equation reads [2], [3]

$$\frac{dL(\boldsymbol{r}, s)}{ds} = -(\sigma_a + \sigma_s)\,L(\boldsymbol{r}, s) + \frac{\sigma_a + \sigma_s}{4\pi}\int_{4\pi} p(s, s') \cdot L(\boldsymbol{r}, s')\,dw' \tag{11}$$

where $L(\boldsymbol{r}, s)$ is the radiance (watt m^{-2} sr^{-1}) at tissue location $\boldsymbol{r}(z, r)$, expressing that $L(\boldsymbol{r}, s)\,dw$ is the amount of light power confined within solid angle dw, moving in the direction s, which crosses a unit area located at $\boldsymbol{r}$. The first term of the r.h.s. of (11) denotes the losses in $L(\boldsymbol{r}, s)$ per unit of length in direction s due to absorption and scattering. The second term denotes the gain in $L(\boldsymbol{r}, s)$ per unit length in direction s due to scattering from all other directions s'. The light power per unit area confined within solid angle dw' coming from direction s' is $L(\boldsymbol{r}, s')\,dw'$ with scattering probability density function $p(s, s')$ for scattering from direction s' to direction s. Note that the transport equation is a *local* equation that considers the spatial balance of light power at coordinate $\boldsymbol{r}$.

To our knowledge, no analytical solution or reasonable approximation is available to (11) for $\sigma_a \sim \sigma_s$ for an incident finite laser beam. Such solutions are now available, however, from Monte Carlo numerical techniques; see, e.g., Wilson and Adam [17] and Keijzer *et al.* [18].

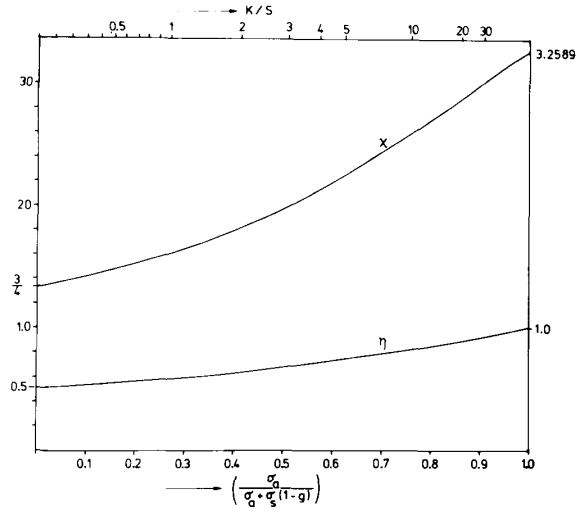

Fig. 5. Parameters η and χ, according to $\sigma_a = \eta K$ and $\sigma_s(1 - g) = \chi S$, as a function of $\sigma_a/[\sigma_a + \sigma_s(1 - g)]$ (lower scale) and K/S (upper scale). The phase function used in the derivation is according to (2d).

Methods to determine σ_a, σ_s, and $p(s, s')$ or g when $\sigma_a \sim \sigma_s$ have not received the attention that has been given to the conditions $\sigma_a >> \sigma_s$. Chandrasekhar [2, p. 19] has solved (11) under the constraint of no collimated or diffuse source (or, if there is such a source, it is expected to be so far away that attenuation of the source has virtually been complete). He has assumed isotropic scattering or $p(s, s') =$ constant, (2a) and Fig. 2(a). It is also easy to show that this solution for isotropic scattering can be extended when the phase function involving strongly forward and isotropic scattering can be represented by the phase function of (2d). In this case, σ_s in Chandrasekhar's solution is replaced by $\sigma_s(1 - g)$ [15]. Once again, parameters K and S can be determined by similar integrating sphere methods using the relations in (9). Here, K and S are related to σ_a and $\sigma_s(1 - g)$ by

$$\sigma_a = \eta K \tag{12a}$$

$$\sigma_s(1 - g) = \chi S \tag{12b}$$

where curves for η and χ are shown in Fig. 5 as a function of $\sigma_a/[\sigma_a + \sigma_s(1 - g)]$ and of K/S. Equations (12) have originally been proposed by Klier [19] for isotropic scattering ($g = 0$). Klier's analysis used the observation that Chandrasekhar's and Kubelka-Munk's formulas for transmission and reflection coefficients were formally identical functions of the optical parameters involved. Equating these coefficients resulted in (12) and Fig. 5. Again, measurement of the collimated attenuation coefficient σ_t yields

$$\sigma_t = \sigma_a + \sigma_s \tag{12c}$$

indicating that σ_a, σ_s, and g can be determined albeit under the constraint that the phase function of (2d) applies.

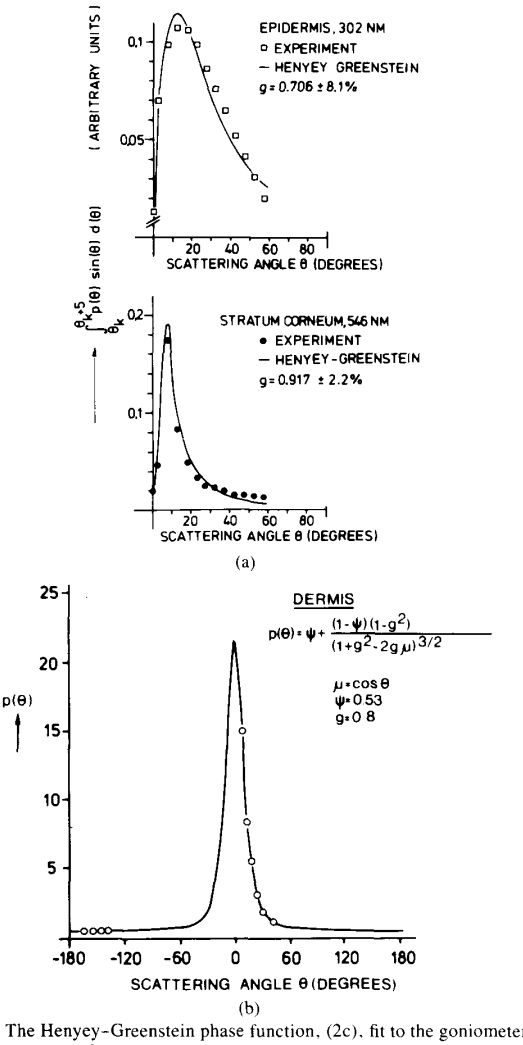

Fig. 6. The Henyey-Greenstein phase function, (2c), fit to the goniometer measurements of Bruls [20] on stratum corneum and epidermis and of Jacques *et al.* [11] and Prahl (S. A. Prahl: three-dimensional calculations of light distributions in tissue, The University of Texas at Austin, 1986, unpublished) on dermis. The measurements by Bruls [20, Fig. 7 and Table I] refer to $\int_{\theta_k}^{\theta_k+5^\circ} p(\theta) \sin\theta d\theta$, with θ_k varying between $\theta_1 = 0$, $\theta_2 = 5°$, $\theta_3 = 10°$, etc.

The authors are not aware that such measurements under these conditions of $\sigma_a \sim \sigma_s$ have been published. These measurements would also require special boundary conditions that may not be easy to realize in practice. Nevertheless, this method is used below to analyze published transmission and reflection data of skin layers in terms of transport equation parameters.

Compilation of Experimental Skin Data

The following paragraphs describe optical properties of skin layers, from measurements performed in a number of different laboratories. No attempt has been made to incorporate the effect of tissue preparations and tissue con-

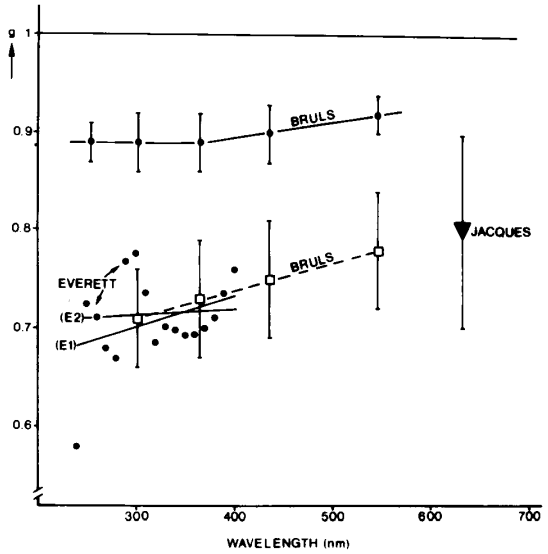

Fig. 7. Compiled experimental g values for: stratum corneum (●) from experimental data by Bruls [20]; and Everett *et al.* [21]; epidermis (□), from data by Bruls [20], and dermis (▼), from Jacques *et al.* [11]. The analyzed data from Everett *et al.* show considerable scatter. A least squares analysis of that data, according to $g = A + B\lambda$ (wavelength λ in nanometers) shows: $A = 0.603$; $B = 3.23 \times 10^{-4}$, see line ($E1$). Neglecting, as Diffey [1] did the point at 240 nm yields: $A = 0.692$; $B = 6.7 \times 10^{-5}$, see line ($E2$), or an almost wavelength independent g value of about 0.715 (250–400 nm), in reasonable correlation with $g = 0.68$ deduced from Diffey's $\beta = 0.84$.

ditions (e.g., the amount of blood in the tissue), upon the reported values.

Stratum Corneum

Bruls [20] published goniometer measurements of *in vitro* stratum corneum. We used a least squares fit to analyze his data according to the Henyey–Greenstein phase function, (2c), extracting values of g (see Fig. 6). The results of g as a function of wavelength shown in Fig. 7 indicate that g is approximately 0.9 with a tendency to increase with increasing wavelength. Stratum corneum is a highly forward scattering layer but, more importantly, the Henyey–Greenstein phase function seems a good description for stratum corneum scattering behavior, see Fig. 6.

Everett *et al.* [21] measured collimated and diffuse transmission, and diffuse reflection from a 10 μm thick sample of "90 percent pure" stratum corneum, in the UV. Figs. 7 and 8 show the analyzed data for g and σ_a, σ_s, respectively, obtained using (12). Values of g found in this way are between 0.58 and 0.78 for wavelengths between 240 and 400 nm, so substantially lower than those derived from Bruls' data. A clear explanation of this discrepancy is not easy to give. However, as it is unknown whether Everett *et al.* used diffuse incidence or collimated incidence in their experiments, it seems at present that Bruls' data are more reliable. Recently, Diffey [1] also used these data by Everett to analyze the optical properties of stratum corneum using a strictly one-dimensional form of (11). The parameter β occurring in Diffey's analysis, describing the fraction of scattered light that is scattered in the forward direction [22], is then related to g by $g = 2\beta - 1$. Diffey's results of σ_a and σ_s, assuming $\beta = 0.84$ (or $g = 0.68$), are consistent with the results given in Figs. 7 and 8.

Epidermis

Goniometer measurements by Bruls [20] on epidermis were again analyzed according to the Henyey–Greenstein phase function (Fig. 6) yielding g values as a function of wavelength (Fig. 7). Again, the Henyey–Greenstein phase function fits well for epidermis, with values between 0.71 at 300 nm and 0.78 at 540 nm, varying linearly with wavelength.

Wan *et al.* [24] published epidermal diffuse integrating sphere measurements of K and S, see (9). Again using these values in conjunction with (12) and Fig. 5 leads to values of σ_a and $\sigma_s(1 - g)$. Assuming that the g values deduced from Bruls' experiments (assuming Henyey–Greenstein phase function behavior) also fit the analysis of (12) and assuming (2d) as the phase function, gives values for σ_s as well. The results are shown in Fig. 8. The epidermis is thus a strongly forward scattering layer with reasonable absorption in the visible but with substantial absorption in the UV. At all wavelengths considered, scattering coefficients appear larger than the corresponding absorption coefficients.

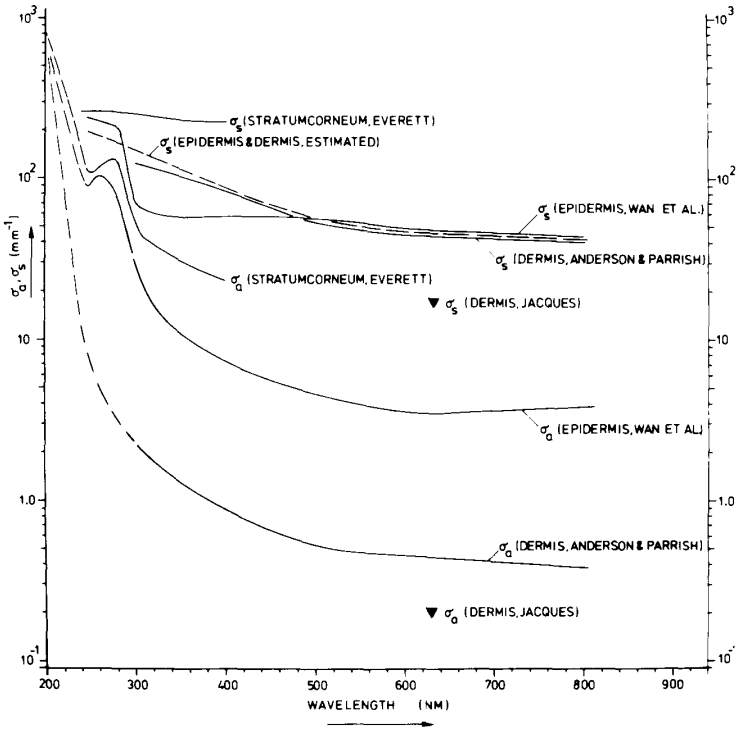

Fig. 8. Experimental absorption (σ_a) and scattering (σ_s) coefficients for stratum corneum (from data by Everett *et al.* [21]); epidermis (from data by Wan *et al.* [23]); and dermis (from data by Anderson and Parrish [25]; and from Jacques *et al.* [11]). For shorter UV wavelengths (<200 nm) absorption coefficients indicated by (— — — —) are likely to reach values of $\sigma_a \sim 1000$ mm^{-1}. The dashed line (----------) shows the estimated epidermal and dermal scattering coefficient, assumed equal to each other.

Dermis

Values for K and S of dermal tissue, obtained from integrating sphere measurements were published by Anderson and Parrish [25]. Conversion of Kubelka–Munk coefficients to transport parameters using (12a) and (12b) yields values for σ_a and $\sigma_s(1 - g)$. Assuming g values vary with wavelength according to Fig. 7 it is possible to compute σ_s with (12b). These values for σ_s as a function of wavelength are illustrated in Fig. 8.

Discussion

Experimental Data

The experimental g value presented in Fig. 7 suggest that skin layers are strongly forward scattering media for wavelengths between 240 and 633 nm. The g values of stratum corneum, analyzed from Everett's reflection and transmission data, show values that are more than 20 percent lower than those from Bruls' data. However, the trend as a function of wavelength is similar within measurement accuracy. The low g value at 240 nm may be an experimental artefact caused by the combined influence of the strong increase in stratum corneum absorption at 240 nm, and experimental difficulties associated with these short UV wavelengths.

Interestingly, the dermal g values at 633 nm, from Jacques, is virtually identical to the extrapolated epidermal g factors from Bruls. In addition, these two goniometer experiments show a good fit to the Henyey–Greenstein phase function, (3c) and Fig. 6. As a result, epidermal and dermal g factors may be considered identical according to (wavelength λ in nanometer)

$$g_e \sim g_d \sim 0.62 + \lambda 0.29 \times 10^{-3} \ (\lambda \text{ in nm}). \quad (13)$$

Equation (13) may be used in practice until more goniometer data become available, preferably for skin layers from the same human skin samples. Equation (13) has also been used to analyze dermal σ_s values as a function of wavelength, shown in Fig. 8.

The absorption (σ_a) and scattering (σ_s) coefficients of Fig. 8 show that σ_s is always larger than σ_a for the wavelengths considered (full lines in Fig. 8). The epidermal (and stratum corneum) absorption coefficients show a strong maximum around 260 to 280 nm. This strong increase in σ_a in conjunction with the corresponding increased experimental inaccuracies in the diffuse transmittance and reflectance measurements is probably the reason

TABLE I
WAVELENGTH BANDS (IN NANOMETERS) FOR WHICH BEER'S LAW, (4), AND THE DIFFUSION MODEL, (7), ARE "REASONABLE" OR "GOOD" APPROXIMATIONS TO THE TRANSPORT EQUATION (11). CRITERIA FOR "REASONABLE" AND "GOOD" ARE GIVEN IN THE TEXT. WAVELENGTH BANDS FOR WHICH THE EXACT SOLUTION TO (11) IS *REQUIRED* ARE INDICATED IN THE LAST COLUMN

Skin-Layer	Beer's Law		Diffusion Model		Exact Solution Required
	"Reasonable"	"Good"	"Reasonable"	"Good"	
Epidermis	200–220 nm				220–2000 nm
Dermis	200–220 nm		220–300 nm	300–2000 nm	

that also the measured epidermal scattering coefficient increases strongly at 300 nm. This interpretation, and the observation in Fig. 8 that epidermal and dermal σ_s values virtually coincide between 500 and 633 nm, suggests the dashed curve in Fig. 8 may be a reasonable estimate for both epidermal and dermal scattering coefficients until more data become available. The dermal value of σ_s at 633 nm, from recent work by Jacques, may be the first of such additional data. The discrepancy by a factor of 2.4 is not alarming. Dermal absorption coefficients are about ten times smaller than those for epidermis. Again, Jacques' recent value at 633 nm is lower by a factor of 2.3. The σ_a, σ_s values for stratum corneum, from Everett *et al.*, deviate somewhat from the other (epidermal and dermal) results except for the UV wavelengths around 250 nm. The reason is not clear although it may reflect experimental uncertainties. Fig. 8 incorporates (expected) increase in tissue absorption coefficients towards (an estimated) $\sim 1000\ \text{mm}^{-1}$ for wavelengths < 200 nm (dashed lines).

An interesting question is for what wavelength bands the approximate solutions to the transport equation (11) can be used. First, $\sigma_a >> \sigma_s$ yields Beer's law, (4). We assume $\sigma_a > 10\sigma_s$ yields a good approximation and $\sigma_a > 5\sigma_s$ yields a reasonable approximation to (11). Similarly, the diffusion model (7) yields a good, respectively reasonable approximation to (11) when $\sigma_s(1 - g) > 10\sigma_a$ or $\sigma_s(1 - g) > 5\sigma_a$. Table I has been tabulated from Fig. 8 according to these criteria. Surprisingly, Table I suggests that a better approximation of the transport equation is required for epidermal tissue optics for almost all wavelengths of interest. For the short UV wavelengths (<200 nm) one would intuitively expect Beer's law to apply. However, our analysis shows that Beer's law is only a "reasonable" model. For dermal tissue optics, the diffusion model seems adequate for $\lambda > 220$ nm, and Beer's law "reasonable" for the 200–220 nm band. Attempts to evaluate the accuracy of the diffusion approximation for computed fluxes, radiances, and fluence rates as a function of optical parameters has been recently described [26], [27].

Theoretical Methods

The method [see (12)], employed in this paper to determine transport equation absorption (σ_a) and scattering (σ_s, g) parameters from published data on collimated transmission and diffuse transmission and reflection of a slab of tissue, is exact in principle. However, a condition is that the theoretical boundary conditions can be satisfied experimentally. Another condition is that the phase function of the tissue can be represented by the sum of an isotropic and a strongly forward peaked component, (2d) and Fig. 2(d). Although certain tissues and tissue phantoms indeed show this behavior; see, e.g., the paper by Flock *et al.* [14], available goniometer data of skin layers show their phase functions to be represented quite reasonably by the Henyey–Greenstein phase function, (3c) and Figs. 2(c) and 6. These two phase functions have only their first two moments in common, (3), and Fig. 2(c) and (d) show the substantial difference between them for $g = 0.7$. This strongly suggests the need of theoretical relations, comparable to those of (12), for a Henyey–Greenstein phase function. Most likely, Chandrasekhar's approach [2, p. 19] will work here, transforming the transport integro-differential equation into an easier solvable integral-equation [23, (43)–(47)]. Again, as with (12), this method yields better results only if the theoretical boundary conditions can be satisfied experimentally, which may be difficult.

Summarizing therefore, the optical properties of the skin layers, compiled from different sources and shown in Figs. 7 and 8, can only be considered as approximations, although, most likely, the best values available today. In any case, these results stress both the need for theoretically sound methods and corresponding adequate measurements, as well as the dearth of current reliable optical data of skin layers.

REFERENCES

[1] B. L. Diffey, "A mathematical model for ultraviolet optics in skin," *Phys. Med. Biol.*, vol. 28, pp. 647–657, 1983.
[2] S. Chandrasekhar, *Radiative Transfer.* New York: Dover, 1960.
[3] A. Ishimaru, *Wave Propagation and Scattering in Random Media, Vol. 1.* New York: Academic, 1978.
[4] L. G. Henyey and J. L. Greenstein, "Diffuse radiation in the galaxy," *Astrophys. J.*, vol. 93, pp. 70–83, 1941.
[5] H. C. van de Hulst, *Multiple Light Scattering: Tables, Formulas and Applications, Vol. 2.* New York: Academic, 1980.
[6] R. A. J. Groenhuis, H. A. Ferwerda, and J. J. Ten Bosch, "Scattering and absorption of turbid materials determined from reflection measurements. I: Theory," *Appl. Optics*, vol. 22, pp. 2456–2467, 1983.
[7] M. Keijzer, W. M. Star, and P. R. M. Storchi, "Optical diffusion in layered media," *Appl. Optics*, vol. 27, pp. 1820–1824, 1988.
[8] J. P. A. Marijnissen and W. M. Star, "Phantom measurements for light dosimetry using isotropic and small aperture detectors," in *Por-*

phyrin Localization and Treatment of Tumors, D. R. Doiron and C. J. Gomer, Eds. New York: Alan Liss, 1984, pp. 133–148.

[9] J. P. A. Marijnissen, W. M. Star, J. L. van Delft, and N. A. P. Franken, "Light intensity measurements in optical phantoms and *in vivo* during HPD-photoradiation treatment using a miniature light detector with isotropic response," in *Photodynamic Therapy of Tumors and Other Diseases*, G. Jori and C. Perria, Eds. Padova: Libreria Progetto, 1985, pp. 387–390.

[10] M. J. C. van Gemert, A. J. Welch, W. M. Star, M. Motamedi, and W. F. Cheong, "Tissue optics for a slab geometry in the diffusion approximation," *Lasers Med. Sci.*, vol. 2, pp. 295–302, 1987.

[11] S. L. Jacques, C. A. Alter, and S. A. Prahl, "Angular dependence of He-Ne laser light scattering by human dermis," *Lasers Life Sci.*, vol. 1, pp. 309–333, 1987.

[12] M. J. C. van Gemert, G. A. C. M. Schets, M. Bishop, W. F. Cheong, and A. J. Welch, "Optics of tissue in a multi-slab geometry," *Lasers Life Sci.*, vol. 2, pp. 1–18, 1988.

[13] M. J. C. van Gemert, W. J. de Kleijn, and J. P. Hulsbergen Henning, "Temperature behavior of a model portwine stain during argon laser coagulation," *Phys. Med. Biol.*, vol. 27, pp. 1089–1104, 1982.

[14] S. T. Flock, B. C. Wilson, and M. S. Patterson, "Total attenuation coefficients and scattering phase functions of tissues and phantom materials at 633 nm," *Med. Phys.*, vol. 14, pp. 835–841, 1987.

[15] M. J. C. van Gemert and W. M. Star, "Relations between the Kubelka-Munk and the transport equation models for anisotropic scattering," *Lasers Life Sci.*, vol. 1, pp. 287–298, 1987.

[16] S. L. Jacques and S. A. Prahl, "Modeling optical and thermal distributions in tissue during laser irradiation," *Lasers Surg. Med.*, vol. 6, pp. 494–503, 1987.

[17] B. C. Wilson and G. A. Adam, "A Monte Carlo model for the absorption and flux distributions of light in tissue," *Med. Phys.*, vol. 10, pp. 824–830, 1983.

[18] M. Keijzer, S. L. Jacques, S. A. Prahl, and A. J. Welch, "Light distributions in artery tissue: Monte Carlo simulations for finite diameter laser beams," *Lasers Surg. Med.*, vol. 9, pp. 148–154, 1989.

[19] K. Klier, "Absorption and scattering in plane parallel turbid media," *J. Opt. Soc. Amer.*, vol. 62, pp. 882–885, 1972.

[20] W. A. G. Bruls and J. C. van der Leun, "Forward scattering properties of human epidermal layers," *Photochem. Photobiol.*, vol. 40, pp. 231–242, 1984.

[21] M. A. Everett, E. Yeargers, R. M. Sayre, and R. L. Olsen, "Penetration of epidermis by ultraviolet rays," *Photochem. Photobiol.*, vol. 5, pp. 533–542, 1966.

[22] J. T. Atkins, "Absorption and scattering of light in turbid media," Ph.D. dissertation, Univ. Delaware, June 1965.

[23] W. M. Star, J. P. A. Marijnissen, and M. J. C. van Gemert, "Light dosimetry in optical phantoms and in tissues. I. Multiple flux and transport theory," *Phys. Med. Biol.*, vol. 33, pp. 437–454, 1988.

[24] S. Wan, R. R. Anderson, and J. A. Parrish, "Analytical modeling for the optical properties of the skin with *in vitro* and *in vivo* applications," *Photochem. Photobiol.*, vol. 34, pp. 493–499, 1981.

[25] R. R. Anderson and J. A. Parrish, "Optical properties of human skin," in *The Science of Photomedicine*, J. D. Regan and J. A. Parrish, Eds. New York: Plenum, 1982, pp. 147–194.

[26] G. Yoon, S. A. Prahl, and A. J. Welch, "Accuracies of the diffusion approximation and its similarity relations for laser irradiated biological media," *Appl. Optics*, vol. 28, pp. 2250–2255, 1989.

[27] S. A. Prahl, "Light transport in tissue," Ph.D. dissertation, Univ. Texas, Austin, TX, Dec. 1988.

M. J. C. van Gemert was born in Delft, The Netherlands, on March 25, 1944. He received the M.Sc. degree from Delft University in 1969, and the Ph.D. degree from Leiden University, The Netherlands, in 1972, both in physics.

He was with Philips Research Laboratories, Eindhoven, The Netherlands, as a member of the Gaseous Electronics Group from 1972 to 1978. From 1978 to 1987, he worked as a clinical physicist at St. Joseph Hospital, Eindhoven. He was on leave during 1984–1985 and joined A. J. Welch's research group at The University of Texas at Austin supervising various projects on laser applications in medicine. Since July 1987, he has been working as director of the Experimental Laser Unit of the Academic Medical Centre, University of Amsterdam, The Netherlands.

Steven L. Jacques was born in Spokane, WA, in 1950. He received the B.S. degree in biochemistry from Massachusetts Institute of Technology, Cambridge, the M.S. degree in electrical engineering, and the Ph.D. degree in biophysics, both from the University of California, Berkeley.

He worked for five years at the Wellman Laboratory for Photomedicine, Massachusetts General Hospital, Boston, MA, and attained the rank of Instructor in Dermatology (Biomedical Engineering) at Harvard Medical School. He now is Director of the Laser Biology Research Laboratory and Assistant Professor of Urology at the University of Texas M.D. Anderson Cancer Center, Houston.

H. J. C. M. Sterenborg received the M. S. degree in physics at the Eindhoven University of Technology in 1982 and the Ph.D. degree from the Rijks Universiteit Utrecht in 1987. His Ph.D. work concerned the action spectrum of UV-carcinogenesis.

Currently he is working at the Laser Centre of the Academic Hospital of the University of Amsterdam. His present research interests are tissue optics, laser diagnostics, lithotripsy, and photodynamic therapy.

W. M. Star received the Ph.D. degree in low temperature solid state physics in 1971 from the University of Leiden. He did postdoctoral research at the Francis Bitter National Magnet Laboratory of MIT, Cambridge, MA.

Since 1974 he has been a clinical physicist in radiotherapy at the Dr. Daniel den Hoed Cancer Center in Rotterdam, The Netherlands. Since 1979 he has become increasingly involved in research on Photodynamic Therapy and tumor imaging with exogeneous photosensitizers. This includes animal studies, light delivery, and light dosimetry and clinical applications.